Computers & Structures Vol. 15, No. 4, pp. 481–488, 1982
Printed in Great Britain.

0045-7949/82/040481-08$03.00/0
© 1982 Pergamon Press Ltd.

COMPUTATION OF STRESSES IN A STEAM TURBINE CASING DURING LIFTING

M. S. HAMID† and S. K. BHARGAVA
Corporate Research and Development Division, Bharat Heavy Electricals Ltd., Hyderabad, 500593, India

(*Received* 9 *March* 1981; *received for publication* 14 *December* 1981)

Abstract—The finite element method, using flat shell elements, is applied for determining the stress levels induced in a typical steam turbine casing due to its self weight. Computer programs have been developed for the analysis and frontal solution technique with diagonal pivoting has been used for the solution of the finite element equations. Various loading histories corresponding to different orientations of the casing during mechanical handling were considered in the analysis. The results of the analysis were compared with limited amount of experimental data and were found to be in good agreement.

INTRODUCTION

Generally, a medium sized thermal power plant, has a high pressure turbine, an intermediate pressure turbine and a low pressure turbine. In each turbine, the steam expands and the thermal energy is converted to mechanical energy for driving the generators to produce electricity. The flow diagram of a typical plant is shown in Fig. 1. Each turbine has a rotor wherein the deflector nozzles, diaphragms, bearings, etc. are housed. In case of the low pressure turbine, the casing is a very large structure, since it has to support heavy rotor assemblies and to handle voluminous amount of steam. A typical LP casing for a medium range plant weighs around 30 tons. The bottom half of the casing is shown in Fig. 2 and weighs around 20 tons. It consists of stiffeners, side plates, conical shell to house the rotor and lifting lugs. The various parts of the casing are fabricated separately and are welded together in a particular sequence. This assembled casing is transported from the final assembly shop floor to the site. During lifting of this structure, if the proper instructions are not adhered to, such heavy structures are prone to permanent deformations due to high stress caused by its own weight if the stiffeners are inadequate. The permanent deformation would cause difficulty in alignment during erection.

The purpose of this work is to validate the design of one such casing due to the stresses induced during handling and to verify the positioning of the stiffeners. Since the structure is complex in shape with stiffeners connecting the side plates, it is difficult to analyze by conventional method. The Finite Element Method (FEM) has been used for the analysis. The flat shell elements for the side plates and conical portion of the casing and space frame elements for stiffeners are used in finite

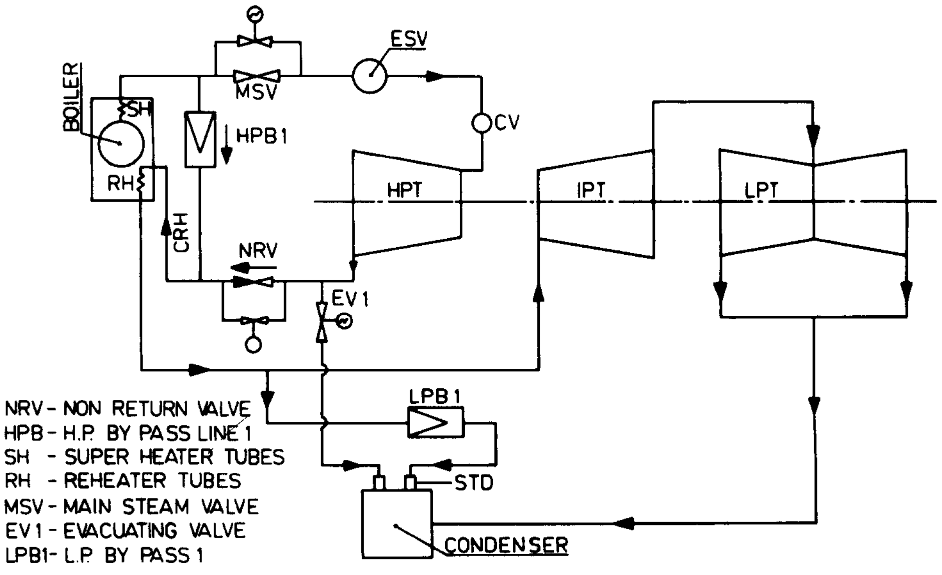

Fig. 1. Flow diagram of a thermal plant.

---

†Currently at Department of Engineering Mechanics, The Ohio State University, Ohio, U.S.A.

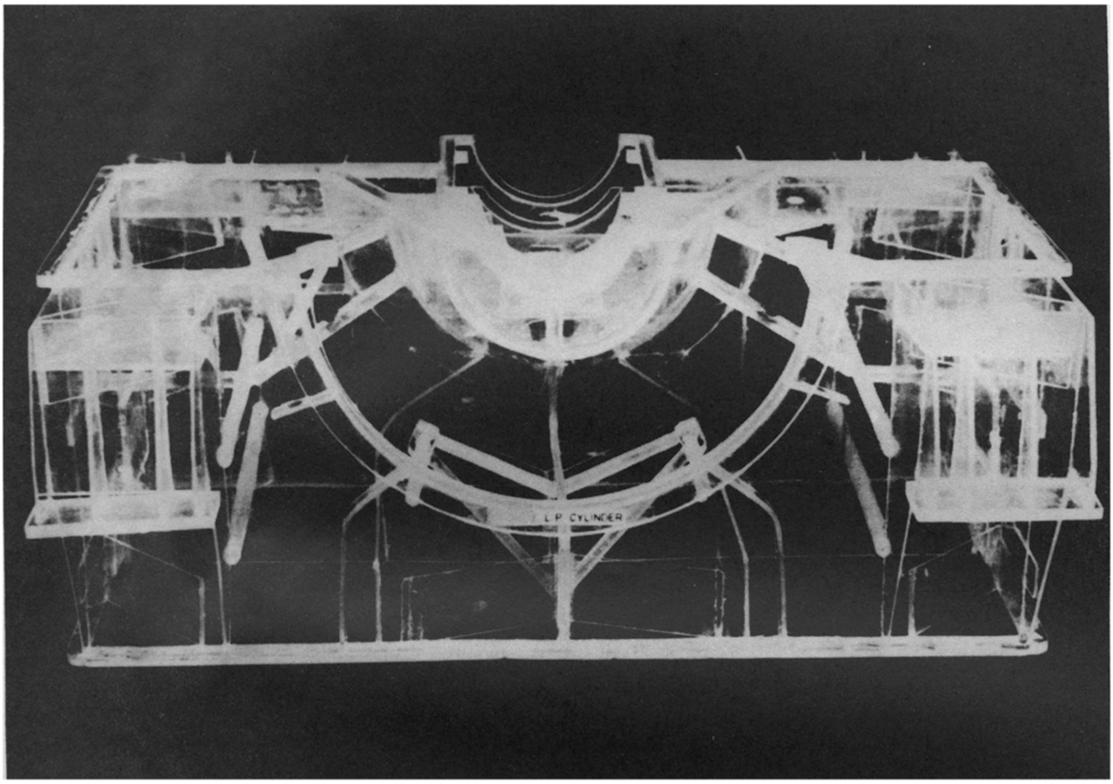

Fig. 2. LP cylinder casing.

element modeling. Three types of loading during lifting are considered for the analysis. The FEM analysis is checked with the available experimental results.

FINITE ELEMENT STRESS ANALYSIS

The LP cylinder casing consists of conical shell and flat plates and bars. Hence, it is considered as a shell structure and is idealized by an assembly of thin flat triangular elements which are assumed to undergo both membrane and bending deformations. The stiffeners are considered as space frame elements with six degrees of freedom at each node.

Element characteristics

The triangular flat element, subject to inplane and bending forces are shown in Fig. 3. It is assumed that the inplane forces do not affect the bending deformation and vice versa[1]. Hence, the inplane stiffness matrix $[K]_p^e$ and bending stiffness matrix $[K]_b^e$ are assumed to be uncoupled. In deriving the element stiffness matrices, linear variation is assumed for the inplane displacements (u, v) and cubic variation is assumed for the normal displacement w. At each node, the displacements u, v, w and rotations θ_x, θ_y and θ_z are taken as unknowns. Area coordinates are used defining the shape function $[N]$ as shown in Fig. 4. The elemental governing stiffness equations are obtained by adding the individual stiffness matrices due to inplane and bending forces.

Elemental stiffness matrixes $[K]_p^e$ *and* $[K]_b^e$. The inplane stiffness matrix $[K]_p^e$ is 6×6 order for the displacements u, v expressed in terms of the nodal displacements as

$$\begin{aligned} u &= N_i u_i + N_j u_j + N_m u_m \\ v &= N_i v_i + N_j v_j + N_m v_m \end{aligned} \tag{1}$$

in which

$$N_i = \frac{a_i + b_i x + c_i y}{2A}$$

$$a_i = x_j y_m - x_m y_j$$

$$b_i = y_j - y_m$$

$$c_i = x_m - x_j$$

and

A = area of the triangle.

The stiffness matrix $[K]_p^e$ is computed from ([1], p. 101)

$$\begin{aligned} [K]_p^e &= \int\int [B]^T[D]_p[B]\,\mathrm{d}x\,\mathrm{d}yt \\ &= [B]^T[D]_p[B]At \end{aligned} \tag{2}$$

wherein $[B]$ is the strain displacement matrix and $[D]$ is the elasticity matrix connecting the stresses $\{\sigma\}$ to the strain $\{\epsilon\}$, i.e.

$$\begin{Bmatrix} \sigma_x \\ \sigma_y \\ \tau_{xy} \end{Bmatrix} = \frac{E}{1-\nu^2} \begin{bmatrix} 1 & \nu & 0 \\ \nu & 1 & 0 \\ 0 & 0 & \frac{1-\nu}{2} \end{bmatrix} \begin{Bmatrix} \epsilon_x \\ \epsilon_y \\ \gamma_{xy} \end{Bmatrix} \tag{3}$$

$$\{\sigma\} = [D]_p\{\epsilon\} \tag{3a}$$

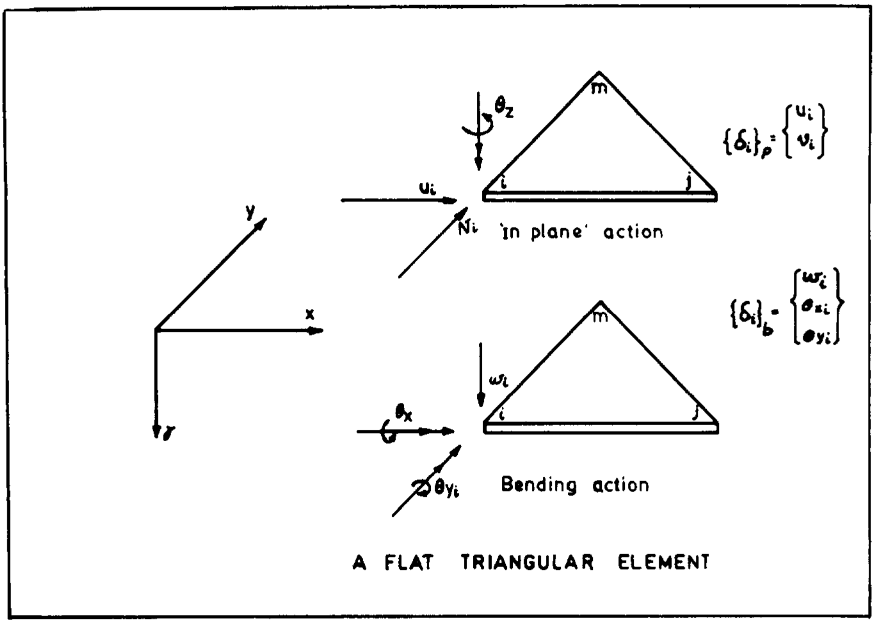
θ_z
m
$\{\delta_i\}_p = \begin{Bmatrix} u_i \\ v_i \end{Bmatrix}$
y
u_i
i
j
v_i
'In plane' action
x
$\{\delta_i\}_b = \begin{Bmatrix} w_i \\ \theta_{xi} \\ \theta_{yi} \end{Bmatrix}$
m
w_i
θ_x
i
j
z
θy_i
Bending action
A FLAT TRIANGULAR ELEMENT

Fig. 3. Area coordinate system.

and

$$\{\epsilon\} = \begin{Bmatrix} \partial u/\partial x \\ \partial v/\partial y \\ \dfrac{\partial u}{\partial y} + \dfrac{\partial v}{\partial x} \end{Bmatrix} = [B]\{\delta\}_p^e \tag{3b}$$

with

$$\{\delta\}_p^e = \begin{Bmatrix} u_i \\ v_i \\ u_j \\ v_j \\ u_m \\ v_m \end{Bmatrix}. \tag{4}$$

The bending stiffness matrix $[K]_b^e$ is 9×9 size and is obtained from displacement function.

$$\begin{aligned} w = {} & \alpha_1 L_1 + \alpha_2 L_2 + \alpha_3 L_3 + \alpha_4(L_1^2 L_2 + \tfrac{1}{2} L_1 L_2 L_3) \\ & + \alpha_5(L_1^2 L_3 + \tfrac{1}{2} L_1 L_2 L_3) + \alpha_6(L_2^2 L_3 + \tfrac{1}{2} L_1 L_2 L_3) \\ & + \alpha_7(L_2^2 L_1 + \tfrac{1}{2} L_1 L_2 L_3) + \alpha_8(L_3^2 L_1 + \tfrac{1}{2} L_1 L_2 L_3) \\ & + \alpha_9(L_3^2 L_2 + \tfrac{1}{2} L_1 L_2 L_3). \end{aligned} \tag{5}$$

The nodal displacements $\{\delta\}^e = [w_i, \theta_{xi}, \theta_{yi}, w_j, \theta_{xj}, \theta_{yj}, w_m, \theta_{xm}, \theta_{ym}]^T$ are written as

$$\{\delta\}_b^e = [C]\{\alpha\}. \tag{6}$$

The generalized strains $\{\epsilon\} = \left[-\dfrac{\partial^2 w}{\partial x^2}, -\dfrac{\partial^2 w}{\partial y^2}, \dfrac{2\partial^2 w}{\partial x \partial y} \right]^T$ in

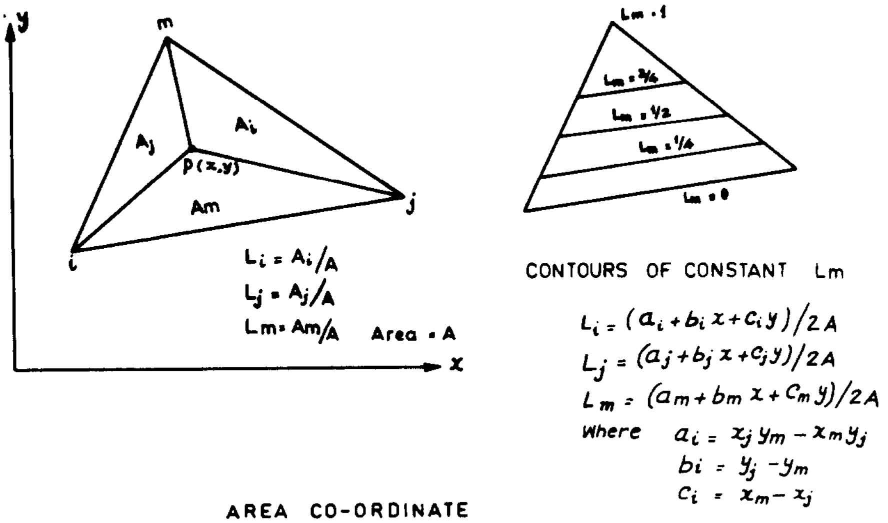

Fig. 4. Flat shell Element.

terms of the nodal displacements are expressed as

$$\begin{aligned}\{\epsilon\} &= [Q]\{\alpha\} \\ &= [Q][C]^{-1}\{\delta\}_b{}^e = [B]\{\delta\}_b{}^e. \end{aligned} \qquad (7)$$

The generalized "stresses" $\{\sigma\} = [Mx, M\dot{y}, Mxy]^T$ and strains are related by the elasticity matrix $[D]_b$ as

$$\{\sigma\} = [D]_b\{\epsilon\}. \qquad (8)$$

The elemental stiffness matrix $K_b{}^e$ is expressed as ([1], p. 236)

$$[K]_b{}^e = [C]^{-1^T}\left(\int\int [Q]^T[D]_b[Q]\,\mathrm{d}x\,\mathrm{d}y\right)[C]^{-1}. \qquad (9)$$

Numerical integration scheme suggested by Cowper[2] has been used to evaluate the matrix $[K]_b{}^e$.

Assembly procedure. The elemental stiffness characteristics are evaluated for each element in its element coordinate system.

The element stiffness equations are of the form

$$\{f\}^e = [K]^e\{a\} \qquad (10)$$

wherein

$$\{f\}_i = \begin{Bmatrix} U_i \\ V_i \\ W_i \\ M_{xi} \\ M_{yi} \\ M_{zi} \end{Bmatrix} \text{ and } \{a\}_i = \begin{Bmatrix} u_i \\ v_i \\ w_i \\ \theta_{xi} \\ \theta_{yi} \\ \theta_{zi} \end{Bmatrix}$$

with element stiffness matrix

$$[K]_{rs} = \left[\begin{array}{cc|ccc|c} \multicolumn{2}{c|}{K^p_{rs}} & 0 & 0 & 0 & 0 \\ \multicolumn{2}{c|}{2\times 2} & 0 & 0 & 0 & 0 \\ \hline 0 & 0 & \multicolumn{3}{c|}{K^b_{rs}} & 0 \\ 0 & 0 & \multicolumn{3}{c|}{3\times 3} & 0 \\ \hline 0 & 0 & 0 & 0 & 0 & 0 \end{array}\right]. \qquad (10a)$$

The elemental stiffness matrix can be transformed to the global system by usual transformation

$$[K]^g_{rs} = [T]^T[K]^e_{rs}[T] \qquad (11)$$

wherein $[T]$ is the transformation matrix.

In the global system, an additional degree of freedom will be present because of the transformation. Compatibility is achieved by inserting null row and column in the stiffness matrix for the coefficients corresponding to the unknown values as in eqn (10a).

If the elements are coplanar, as is the case in this analysis, the final solution will lead to difficulty because of the singularity of the matrix. To circumvent this difficulty, a fictitious set of rotation stiffness coefficients are added in all the elements as suggested by Zienkiewicz[1]. For the triangular element, the fictitious stiffness coefficients are defined as

$$\begin{Bmatrix} M_{zi} \\ M_{zj} \\ M_{zk} \end{Bmatrix} = \alpha Et\Delta \begin{bmatrix} 1 & -0.5 & -0.5 \\ -0.5 & 1 & -0.5 \\ -0.5 & -0.5 & 1 \end{bmatrix} \begin{Bmatrix} \theta_{zi} \\ \theta_{zj} \\ \theta_{zm} \end{Bmatrix} \qquad (12)$$

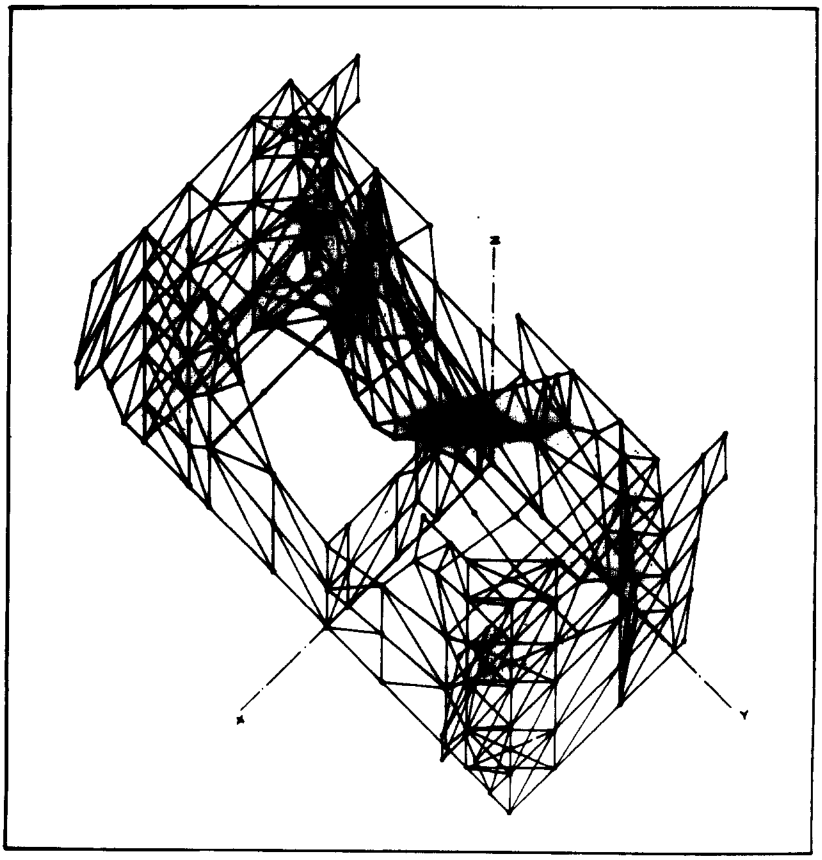

Fig. 5. Finite Element Discretization of LP casing.

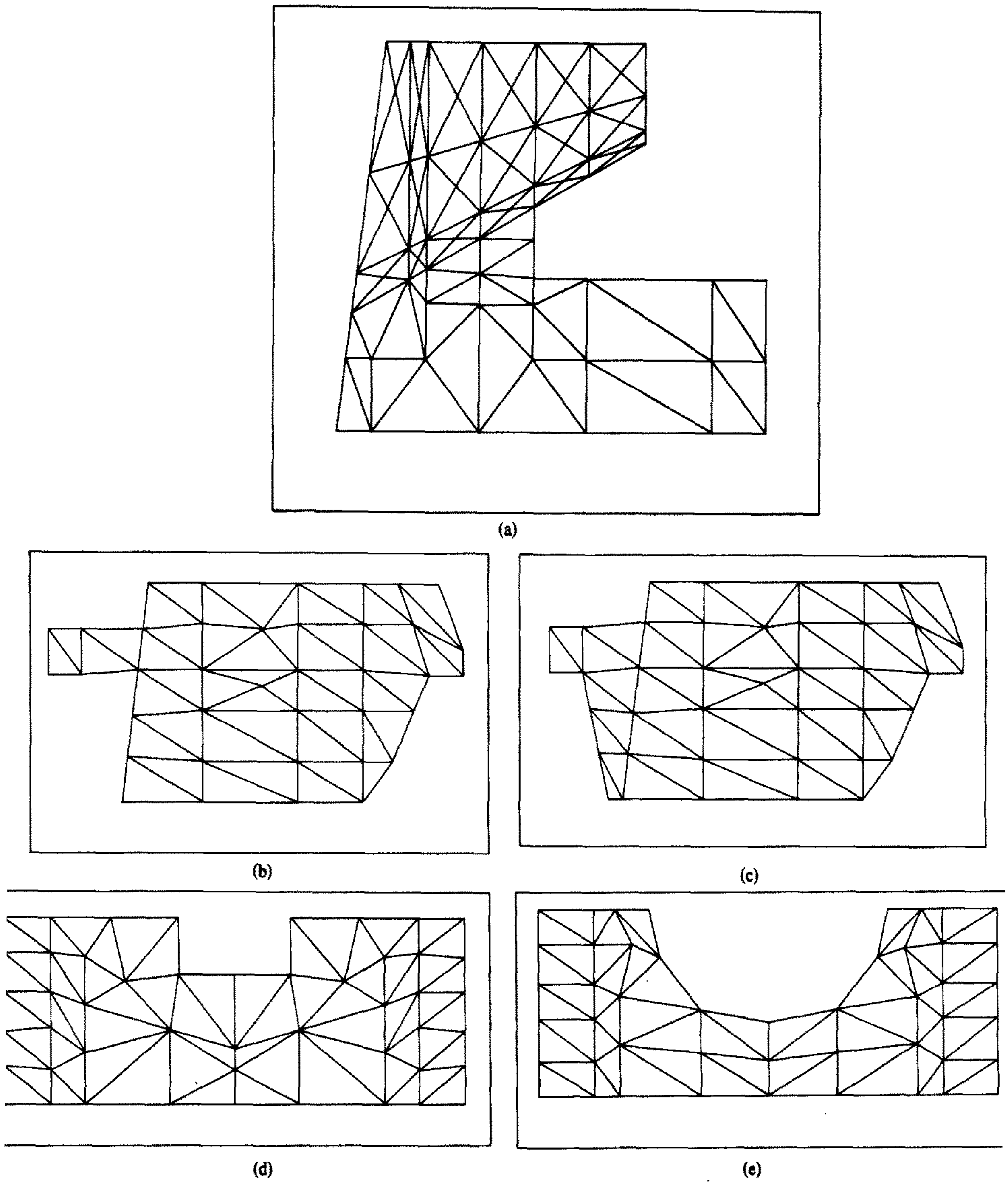

Fig. 6. (a) *FEM Discretization of central support plate with conical shell.* (b) *FEM discretization of side plate I.* (c) *FEM discretization of side plate II.* (d) *FEM discretization of front plate.* (e) *FEM discretization of rear plate.*

wherein α is a coefficient and is taken as 0.03 in the analysis. The stiffness matrix of the stiffener element is given in Appendix 1.

Discretization and solution procedure

Even though the structure is geometrically symmetric about the axis of the turbine, the loadings due to various parts of the assembly, i.e. the weights of the parts which are acting on the conical portion of the casing, are not exactly symmetric. Apart from this small unsymmetric loading, during lifting of the structure, a little tilt would alter the symmetricity. Hence, the complete structure is considered for the analysis. The structural discretization is shown in Fig. 5. The discretization resulted in 438 elements with 1428 degrees of freedom. The data prepared for nodal coordinates, and element connectivity are checked by computer plot. Each individual components such as conical shell and side plates are plotted and they have been checked to avoid any error in data (Fig. 6).

The structure considered in this analysis is a closed one and use of any band solver procedure will be uneconomical with respect to computer memory and the solution of assembly equations. In order to efficiently

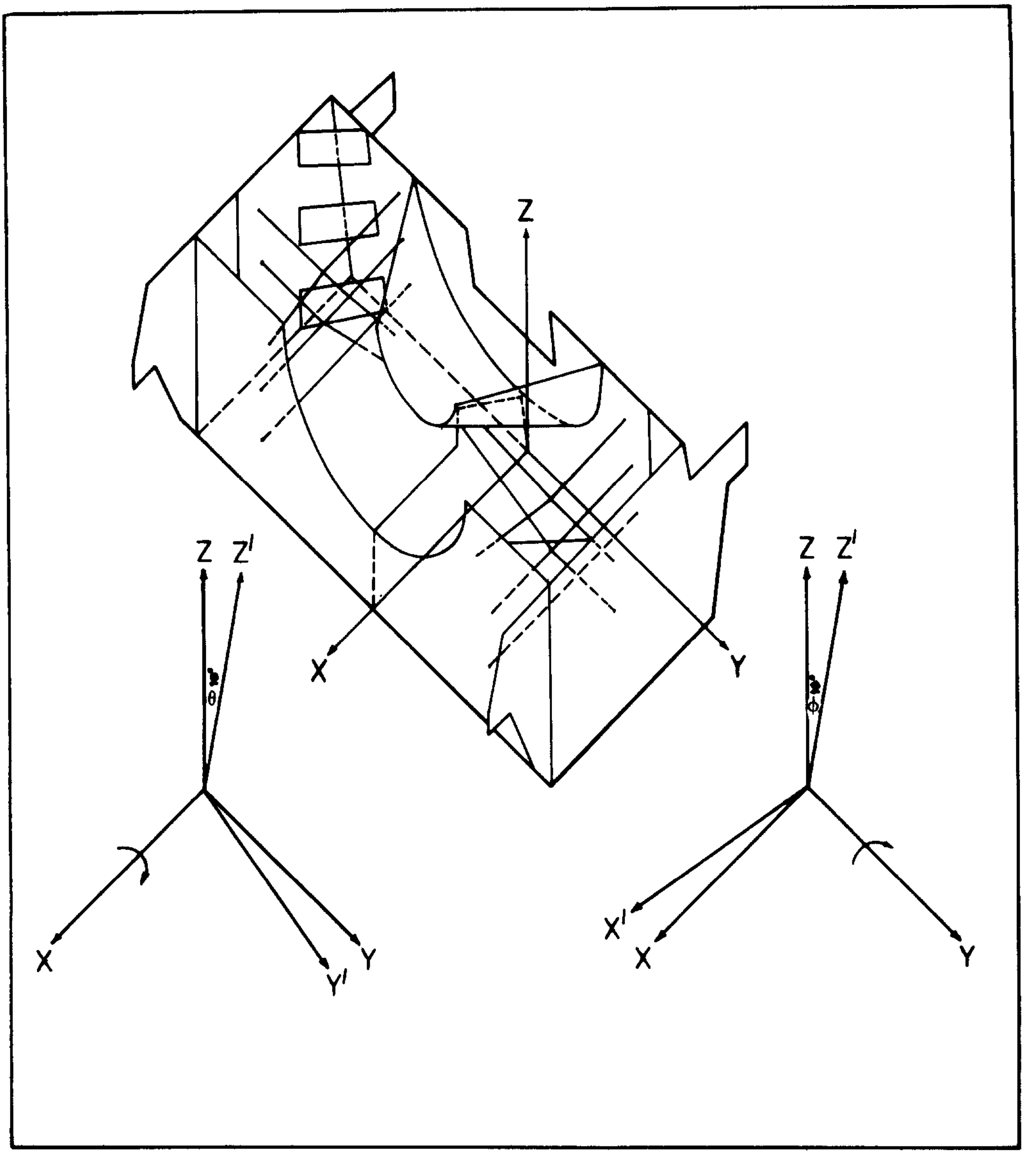

Fig. 7. Loading conditions.

handle the solution of this problem, the frontal solution technique[3] is followed. The frontal solution is advantageous since the solution procedure proceeds based on elementwise elimination. Hence, this is highly suited for the analysis of closed structures and the solution can be obtained with minimal active core memory. The solution procedure presented in [3] has been modified to incorporate the diagonal pivoting during the elimination process. Incorporation of diagonal pivoting permits use of less core and minimizes the input/output operations. Also, after assembly of each element, the nodes which are not appearing further in any other element are eliminated resulting in more space for assembly of the other elements in the solution procedure.

The computer programs developed for this analysis consist of a main program and subroutines for (i) evaluating the element inplane and bending stiffnesses, (ii) frontal solver and (iii) stress computation. The frontal solution routine assembles the element equations and solves for the nodal displacements. The element stresses are computed using the displacements. The stresses in the shell elements due to bending are calculated at the integration points in both the surfaces. The principal stresses are evaluated using the inplane and bending stresses.

The loadings considered for the analysis are (i) the perfect lift, (ii) the casing is tilted by 10° about the turbine axis ($\theta = 10°$) and (iii) the casing is tilted by 10° about the transverse axis ($\phi = 10°$) (Fig. 7).

For each loading, the computer time taken for the analysis is 56 min. of I/O time with 19.5 min. of CPU time in a IBM 370/155 systems with 512 K bytes memory.

The results obtained for various orientation of the casing during lifting are shown in Table 1.

EXPERIMENTAL ANALYSIS

An experiment was carried out in the site on the same casing by strain gauging. The strain gauges were put at selected points as shown in the Fig. 8. The stresses were computed using the strains induced by lifting the actual model. Only selected points were considered because of

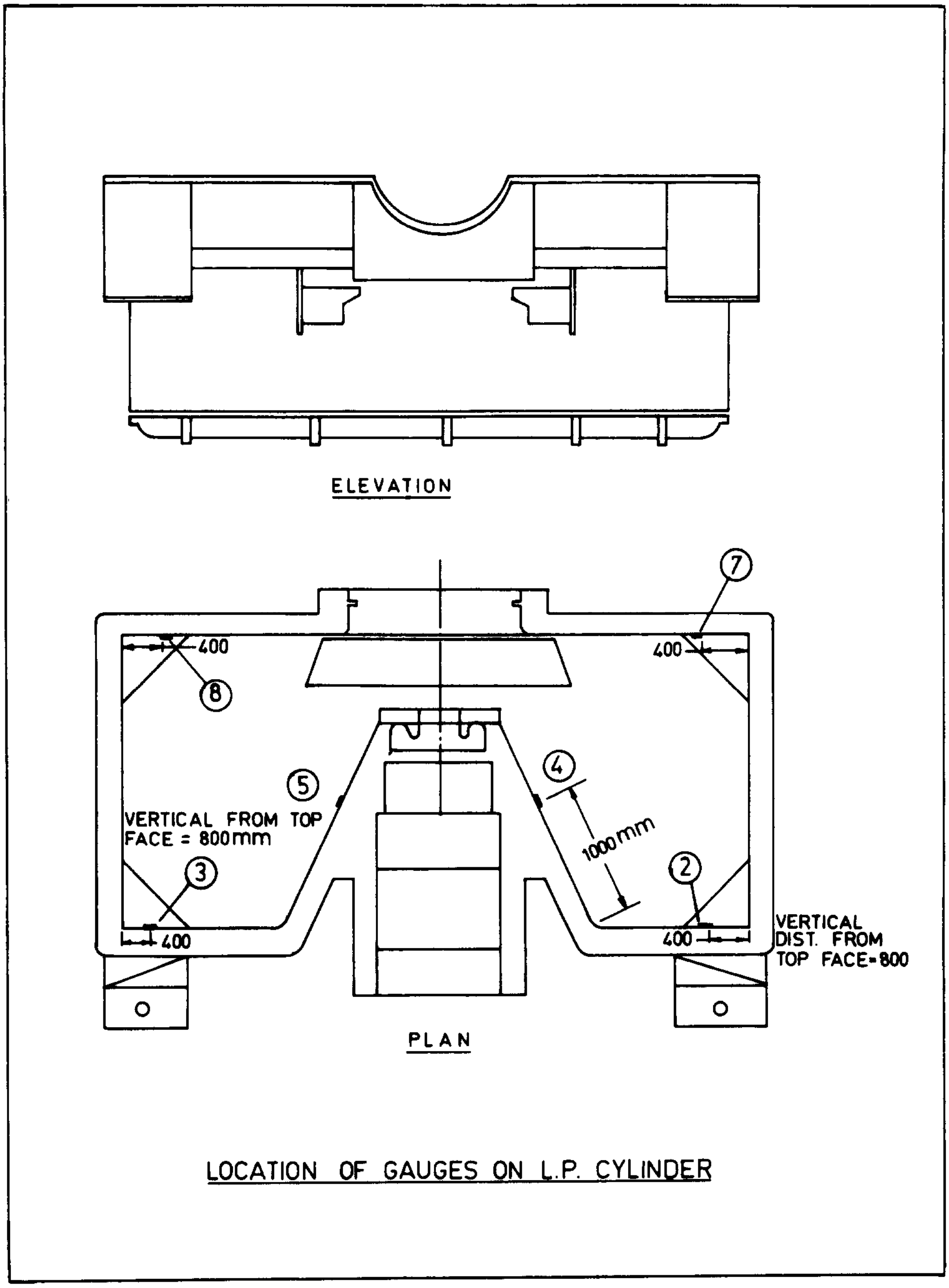

Fig. 8. Position of Strain gauges in LP cylinder.

the restriction due to the capacity of the instrument. The stresses computed were given in Table 1.

Table 1. Comparison of stresses (Kgf/cm^2)

	$\theta = \phi = 0°$		$\theta = 10°$	$\phi = 10°$
Position	FEM	Expl	FEM	FEM
R_2	6.8	6.17	21.09	19.60
R_3	10.7	10.10	23.00	21.00
R_4	2.6	1.98	4.41	5.10
R_5	3.1	3.57	2.41	2.80
R_7	11.2	10.80	26.20	25.1
R_8	12.6	15.10	29.60	39.9

RESULTS AND DISCUSSION

For normal lifting condition for which the experimental results are available, the stresses are evaluated using FEM modeling and a comparison has been shown in Table 1. The variation of the FEM results with the experimental values are 4–30% in some locations. This is due to the lumping of the weights of the various parts which are coming to the conical portion of the casing to house the rotor. However, the results are in good agreement with the experimental values which provide confidence in using the same modeling for different types of loading. For the given stiffener arrangements, the stresses induced during normal lifting of the structure are within the allowable stress values.

In actual practice, a small amount of tilting may occur about the central line of the casing during mechanical handling. This tilting is simulated by simply changing the nodal coordinates. The tilting about turbine and transverse axes have been considered. It is observed that the stresses have reached double the value compared to the normal lifting conditions for a 10° tilt (Table 1). The stresses for this amount of tilt are within admissible limits which validates the stiffener arrangements provided. However, if the stiffeners are inadequate, the stresses will be very high which will result in permanent deformation at certain locations of the casing leading to difficulty in alignment during erection.

CONCLUSION

The design analysis of the LP turbine has been carried out using the finite elements. A flat triangular shell element and bar elements have been chosen in discretizing the casing. The computer code developed uses frontal solution procedure since this is very advantageous for closed type of structures. The analysis has been done for loads which result during lifting of the casing. The computed results have been compared with experimental results and were found to be in good agreement for normal lifting. Using this computer code, one particular arrangement of the stiffeners was checked for stresses which would result during improper lifting of this structure. The stresses induced are within the safe allowable limit indicating that the stiffener arrangements are adequate. The finite element modeling help evaluate the stresses induced in the turbine casing for validating the design. Also, the computer code developed can be used for the design analysis of box type power plant equipment such as condensers, large D.C. and A.C. machine frames, etc.

Acknowledgments—The authors express their gratitude to Dr. A. Gopalakrishnan, General Manager, Corporate Research and Development Division of Bharat Heavy Electricals Ltd., for his encouragement and suggestions throughout the execution of this work. The authors thank the management of BHEL for permitting to publish this work.

REFERENCES

1. O. C. Zienkiewicz, *The Finite Element Method in Engineering Science*. McGraw Hill, London (1977).
2. G. R. Cowper, Gaussian quadrature formulas for triangles. *Int. J. Num. Meth. in Engng* 7, 405–408 (1973).
3. P. Hood, Frontal solution program for unsymmetric matrices. *Int. J. Num. Meth. in Engng* **10**, 379–399 (1976).

APPENDIX

$$
\begin{bmatrix}
\frac{EA}{L} & & & & & & & & & & & \\
0 & \frac{12EI_z}{L^3} & & & & & & & & & & \\
0 & 0 & \frac{12EI_y}{L^3} & & & & & & & & & \\
0 & 0 & 0 & \frac{GJ}{L} & & & & & & & & \\
0 & 0 & \frac{-6EI_y}{L^2} & 0 & \frac{4EI_y}{L} & & & & & & & \\
0 & \frac{6EI_z}{L^2} & 0 & 0 & 0 & \frac{4EI_z}{L} & & & \text{SYMMETRIC} & & & \\
\frac{-EA}{L} & 0 & 0 & 0 & 0 & 0 & \frac{EA}{L} & & & & & \\
0 & \frac{-12EI_z}{L^3} & 0 & 0 & 0 & \frac{-6EI_z}{L^2} & 0 & \frac{12EI_z}{L^3} & & & & \\
0 & 0 & \frac{-12EI_y}{L^3} & 0 & \frac{6EI_y}{L^2} & 0 & 0 & 0 & \frac{12EI_y}{L^3} & & & \\
0 & 0 & 0 & \frac{-GJ}{L} & 0 & 0 & 0 & 0 & 0 & \frac{GJ}{L} & & \\
0 & 0 & \frac{-6EI_y}{L^2} & 0 & \frac{2EI_y}{L} & 0 & 0 & 0 & \frac{6EI_y}{L^2} & 0 & \frac{4EI_y}{L} & \\
0 & \frac{6EI_z}{L^2} & 0 & 0 & 0 & \frac{2EI_z}{L} & 0 & \frac{-6EI_z}{L^2} & 0 & 0 & 0 & \frac{4EI_z}{L}
\end{bmatrix}
$$

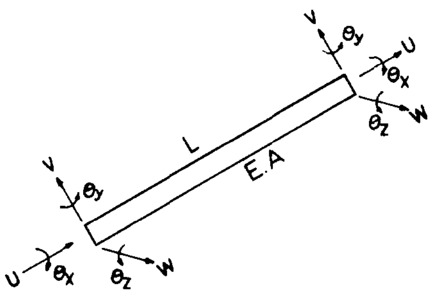

STIFFNESS MATRIX OF SPACE FRAME ELEMENT.